Published in final edited form as:
Development. 2020 January 23; 147(2): . doi:10.1242/dev.177725.

DUX is a non-essential synchronizer of zygotic genome activation

Alberto De Iaco, **Sonia Verp**, **Sandra Offner**, **Delphine Grun**, **Didier Trono***
School of Life Sciences, Ecole Polytechnique Fédérale de Lausanne (EPFL), 1015 Lausanne, Switzerland

Abstract

Some of the earliest transcripts produced in fertilized human and mouse oocytes code for DUX, a double homeodomain protein that promotes embryonic genome activation (EGA). Deleting *Dux* by genome editing at the one- to two-cell stage in the mouse impairs EGA and blastocyst maturation. Here, we demonstrate that mice carrying homozygous *Dux* deletions display markedly reduced expression of DUX target genes and defects in both pre- and post-implantation development, with, notably, a disruption of the pace of the first few cell divisions and significant rates of late embryonic mortality. However, some $Dux^{-/-}$ embryos give rise to viable pups, indicating that DUX is important but not strictly essential for embryogenesis.

Keywords

DUX; Embryonic development; Zygotic genome activation

Introduction

Fertilization of the vertebrate oocyte is followed by transcription of the parental genomes, a process known as zygotic or embryonic genome activation (ZGA or EGA) (Jukam et al., 2017). In zebrafish and *Drosophila*, maternally inherited transcription factors are responsible for this event (Lee et al., 2013; Liang et al., 2008). In placental mammals, the EGA transcriptional program is directly activated at or after the two-cell (2C) stage by a family of transcription factors expressed after fertilization, the DUX proteins (De Iaco et al., 2017; Hendrickson et al., 2017; Whiddon et al., 2017). Recent studies suggest that DPPA2 and DPPA4 are maternal factors responsible in the mouse for DUX expression and downstream target activation, although this model still needs to be validated *in vivo* (De Iaco et al., 2019;

*Author for correspondence (didier.trono@epfl.ch).
iDA.D.I., 0000-0001-8388-4304
D.T., 0000-0002-3383-0401

Competing interests
The authors declare no competing or financial interests.

Author contributions
Conceptualization: A.D.I., D.T.; Methodology: A.D.I., S.V., S.O., D.G.; Investigation: A.D.I., S.V., S.O.; Data curation: A.D.I., D.G.; Writing - original draft: A.D.I.; Writing - review & editing: D.T.; Supervision: D.T.; Funding acquisition: D.T.

Data availability
RNA-seq data have been deposited in Gene Expression Omnibus under accession number GSE141321.

Europe PMC Funders Author Manuscripts

Eckersley-Maslin et al., 2019). Forced expression of DUX proteins in murine or human cell lines triggers the aberrant activation of EGA-restricted genes. Conversely, deleting *Dux* by CRISPR-mediated genome editing before the two-cell stage in murine embryos leads to reduced expression of DUX targets such as *Zscan4* and the transposable element (TE) *MERVL* and severe defects in early development, with many embryos failing to reach the morula/blastocyst stage (De Iaco et al., 2017). However, this procedure also yields some viable mice carrying heterozygous *Dux* deletions. Here, we demonstrate that crossing these $Dux^{+/-}$ animals results in $Dux^{-/-}$ embryos with impaired EGA and severe but not uniformly fatal defects in early development.

Results and Discussion

The murine *Dux* gene is found in tandem repeats of variable lengths in so-called macrosatellite repeats (Leidenroth et al., 2012). We injected zygotes collected from B6D2F1 mothers with sgRNAs directed at sequences flanking the *Dux* locus (Fig. 1A,B), and transferred the resulting products into pseudo-pregnant B6CBA mothers. One out of 42 pups carried a mono-allelic deletion of the targeted region ($Dux^{+/-}$) validated by Sanger sequencing of the junction. This animal was backcrossed twice with wild-type (WT) B6D2F1 mice to ensure germline transmission of the mutation. The resulting $Dux^{+/-}$ mice were healthy and did not display any macroscopic phenotype.

Transcription of *Dux* normally starts in zygotes just after fertilization and stops a few hours later (De Iaco et al., 2017), suggesting that the presence of a functional *Dux* allele is not necessary in germ cells. In our previous work, we demonstrated that inhibition of DUX expression in zygotes impairs early embryonic development. To characterize further the role of DUX, $Dux^{+/-}$ mice were crossed and the frequency of *Dux* mono- and bi-allelic deletions was determined in the progeny (Table 1). There was only a minor deviation from a Mendelian distribution of genotypes, with a slightly lower than expected frequency of $Dux^{-/-}$ pups. Furthermore, adult $Dux^{-/-}$ mice were healthy and had a normal lifespan. To ensure that *Dux* was not expressed from some other genomic locus, the absence of its transcripts was verified in testis of $Dux^{-/-}$ mice, because this is an adult tissue where these RNAs are normally detected (Snider et al., 2010) (Fig. 1C).

To explore further the role of DUX in pre-implantation embryos, we compared the size of litters yielded by isogenic $Dux^{+/+}$ or $Dux^{-/-}$ crossings (Table 2, Fig. 1D). Crosses between $Dux^{-/-}$ mice led to strong reductions in litter size and delayed delivery, and some of the rare pups were eaten by their mother after delivery, probably because they were either stillborn or exhibited physical impairments. Furthermore, some $Dux^{-/-}$ females failed to give any pup, even when crossed with $Dux^{-/-}$ males that had previously demonstrated their fertility when bred with other $Dux^{-/-}$ females (not shown). Because this subgroup of $Dux^{-/-}$ females visually appeared pregnant at the time of expected delivery, we bred them with the same $Dux^{-/-}$ males and examined their uterus at embryonic day (E) 18.5 (Fig. 1E). Surprisingly, we found a significant number of macroscopically normal embryos, suggesting that death occurred around birth. Interestingly, the perinatal lethality was rescued when $Dux^{-/-}$ females were crossed with wild-type males (Fig. 1F). To exclude a role of paternal *Dux* in embryonic

development, we also bred wild-type females with *Dux*$^{-/-}$ males and found normal litter size (Fig. 1G).

We then analyzed whether the strong lethality observed after *Dux*$^{-/-}$×*Dux*$^{-/-}$ crosses occurred before implantation. For this, we repeated isogenic crosses of WT or *Dux*$^{-/-}$ mice, retrieved the zygotes at E0.5 (27 embryos from three WT×WT and 42 embryos from five *Dux*$^{-/-}$×*Dux*$^{-/-}$ crosses), and monitored their *ex vivo* development for 4 days (Fig. 2A). We found that starting at E1.5, *Dux*$^{-/-}$ embryos divided faster than their WT counterparts, yet sometimes unevenly, with formation of three-cell (3C) structures (Fig. 2B). At E2.0, WT embryos caught up whereas *Dux*$^{-/-}$ embryos seemed partially blocked, and exhibited a clear delay at E3.5 with significantly reduced blastocyst formation. By E4.5, only 65% *Dux*$^{-/-}$ embryos reached the blastocyst stage, compared with 100% for WT. Confirming these findings, examination of E3.5 embryos from WT×WT or *Dux*$^{-/-}$×*Dux*$^{-/-}$ crosses revealed a strong delay in blastocyst formation and increased levels of lethality in the absence of DUX (Fig. 2C,D). In conclusion, a subset of embryos derived from *Dux*$^{-/-}$ crosses fails to implant, and the rest generally die around birth.

Finally, we tested the consequences of lack of zygotic DUX on the transcriptional program of 2C-stage embryos. We collected 15 zygotes from three heterozygous *Dux*$^{+/-}$×*Dux*$^{+/-}$ crosses, incubated them *in vitro* and collected RNA 5 h after the formation of 2C embryos. The transcriptomic analysis revealed three embryos with undetectable levels of *Dux* transcripts, indicating that they most likely were *Dux*$^{-/-}$ (Fig. 3A). Interestingly, the three *Dux* RNA-depleted 2C embryos exhibited significant reductions in the expression of genes and TEs (MERVL-int) previously identified as DUX targets, but not of other ZGA-specific genes (Fig. 3B,C) (De Iaco et al., 2017). We then bred one WT and one *Dux*$^{-/-}$ female with males from the same genetic background, and compared the transcription of putative DUX target genes and TEs in the two resulting 2C embryos. Products of the *Dux*$^{-/-}$×*Dux*$^{-/-}$ crosses displayed a strong decrease in the expression of *Dux* and candidate DUX target genes and TEs (Fig. 3D-F). A mild loss of expression of 2C genes that were previously shown to be independent of DUX in mouse embryonic stem cells (mESCs) was also detected.

We further validated these results by collecting 17 zygotes from three heterozygous *Dux*$^{+/-}$×*Dux*$^{+/-}$ crosses, and analyzing gene expression by qPCR (Fig. 4A). All three *Dux* RNA-depleted 2C embryos exhibited significant reductions in the expression of some (MERVL, *Zscan4*, *Eif1a*, *Usp17la*, *B020004J07Rik*, *Tdpoz4* and *Cml2*), but not all *Duxbl*, *Sp110*, *Zfp352* genes previously suggested to represent DUX targets (De Iaco et al., 2017). We then analyzed RNA from seven WT and 11 *Dux*$^{-/-}$ 2C embryos derived from breeding two WT and three *Dux*$^{-/-}$ females with males from the same genetic background (Fig. 4B). Products of the *Dux*$^{-/-}$×*Dux*$^{-/-}$ crosses displayed a clear decrease in the expression of a subset of candidate DUX targets (MERVL, *Zscan4*, *Eif1a*, *Usp17la*, *B020004J07Rik*), whereas others (*Tdpoz4*, *Cml2*, *Duxbl*, *Sp110*, *Zfp352*) were again unaffected.

In summary, the present work confirms that DUX promotes murine embryonic development. In spite of also surprisingly demonstrating that this factor is not absolutely essential for this process, it further reveals that DUX depletion results in a variable combination of pre- and

Europe PMC Funders Author Manuscripts

post-implantation defects, the consequences of which also appear to be cumulative over generations. DUX-devoid embryos originated from homozygous knockout (KO) breeding displayed deregulations in the timing and the ordinance of the first few cell divisions, various degrees of impairments in their ability to become blastocysts, and, for those reaching that stage, high levels of perinatal mortality. Nevertheless, these defects became truly apparent only when DUX was absent already in the oocyte, as the frequency of *Dux*$^{-/-}$ pups derived from the crossing of heterozygous *Dux*$^{+/-}$ parents was only slightly below a Mendelian distribution whereas the resulting *Dux*$^{-/-}$ females yielded markedly reduced progenies, some even appearing sterile when crossed with *Dux*$^{-/-}$ males. However, this defect was completely rescued by zygotic expression of *Dux*, as breeding these *Dux*$^{-/-}$ females with WT males resulted in the production of normal-size litters of pups devoid of obvious defects. Thus, the presence of DUX during only a few hours after fertilization appears to condition not only the conduct of the first few embryonic cell divisions, but also to bear consequences that extend well beyond the pre-implantation period, long after *Dux* transcripts have become undetectable. Our data are in line with the results of two recent studies, both of which found that *Dux* is necessary for normal fertility but is not absolutely essential for mouse development (Chen and Zhang, 2019; Guo et al., 2019). However, while one of these studies (Guo et al., 2019) documented ZGA abnormalities closely resembling those observed in our work, the other (Chen and Zhang, 2019) detected only minimal transcriptional disturbances at this developmental stage. The bases for these differences are unknown, but our finding that the consequences of *Dux* depletion vary from pup to pup and are cumulative over generations indicate both stochasticity in the observed phenotype and its attenuation by compensatory factors that have yet to be identified. Deleting the *Dux* inducers *Dppa2* or *Dppa4* also results in perinatal lethality (Madan et al., 2009; Nakamura et al., 2011), but in this case defects in lung and skeletal development are observed, which correlate with the expression of these two genes later in embryogenesis. Future studies should therefore attempt to characterize better the molecular defects induced by DUX depletion, to explain how the full impact of the *Dux* KO phenotype is only expressed at the second generation, and how even at that point it can be fully rescued by paternally encoded *Dux* zygotic expression.

Materials and Methods

Plasmids

Two single guide RNAs (sgRNAs) targeting sequences flanking the *Dux* macrosatellite repeat (Fig. 1A) were cloned into px330 using a standard protocol. The primers used to clone the sgRNAs have been previously described (De Iaco et al., 2017).

Generation of transgenic mice carrying *Dux*$^{-/-}$ alleles

Pronuclear injection was performed according to the standard protocol of the Transgenic Core Facility of EPFL. In summary, B6D2F1 mice were used as egg donors (6 weeks old). Mice were injected with pregnant mare serum gonadotropin (10 IU), and human chorionic gonadotropin (10 IU) 48 h after. After mating females overnight with B6D2F1 males, zygotes were collected and kept in KSOM medium pre-gassed in 5% CO_2 at 37°C. Embryos were then transferred to M2 medium and microinjected with 10 ng/μg of px330 plasmids

encoding for Cas9 and the appropriate sgRNAs diluted in injection buffer (10 mM Tris HCl pH 7.5, 0.1 mM EDTA pH 8, 100 mM NaCl). After microinjection, embryos were re-implanted in pseudopregnant B6CBA mothers. The pups delivered were genotyped for *Dux* null alleles using previously described primers (De Iaco et al., 2017). The mouse carrying the *Dux* null allele was then bred with B6D2F1 mice to ensure that the transgenic allele reached the germ line and to dilute out any randomly integrated Cas9 transgene. This process was repeated once again to obtain second filial generation (F2) $Dux^{-/+}$ mice.

Breeding experiments

Mice between 6 and 25 weeks old were used for breeding experiments.

Monitoring of pre-implantation embryos

Mothers were superovulated and mated with males as described above. Zygotes were collected and cultured in KSOM medium at 37°C in 5% CO_2 for 4 days. Each embryo was monitored every 12 h to determine the stage of development. When 2C were used for RNA-seq or qPCR, zygotes were monitored every hour until cell division and 5 h later were collected for further analysis. Time-lapse experiments of pre-implantation embryos were carried out in 96-well plates using Operetta CLS High-Content Analysis System for image acquisition. Embryos were checked from zygote to morula every hour.

Randomization and blind outcome assessment were not applied. All animal experiments were approved by the local veterinary office and carried out in accordance with the EU Directive (2010/63/EU) for the care and use of laboratory animals.

Standard PCR, RT-PCR and RNA sequencing

For genotyping the *Dux* null allele, genomic DNA was extracted with DNeasy Blood & Tissue Kits (Qiagen) and the specific PCR products were amplified using PCR Master Mix 2X (Thermo Scientific) combined with the appropriate primers (design in Fig. 1A, previously described; De Iaco et al., 2017). Ambion Single Cell-to-CT kit (Thermo Fisher) was used for RNA extraction, cDNA conversion and mRNA pre-amplification of 2C-stage embryos. Primers (previously listed) were used for SYBR green qPCR (Applied Biosystems) (De Iaco et al., 2017). RNA from 2C embryos was amplified using Smart Seq V4 Ultra Low Input RNA kit (Takara) and library were prepared using Nextera XT DNA Library Prep Kit (Illumina).

RNA-seq dataset processing

RNA-seq of mouse embryo samples was mapped to mm9 genome using hisat2 aligner (Kim et al., 2015) for unstranded and paired-end data with options -k 5 –seed 42 -p 4. Counts on genes and TEs were generated using featureCounts (Liao et al., 2014) with options -p -T 4 -t exon –g.gene_id -Q 10, using a gtf file containing both genes and TEs to avoid ambiguity when assigning reads. For repetitive sequences, an in-house curated version of the mm9 open-3.2.8 version of the Repeatmasker database was used (fragmented LTR and internal segments belonging to a single integrant were merged). Only uniquely mapped reads were used for counting on genes and TEs.

RNA-seq analysis

Normalization for sequencing depth and differential gene expression analysis was performed using the TMM method as implemented in the limma package of Bioconductor (Gentleman et al., 2004), using the counts on genes as library size. TEs overlapping exons or having fewer than one read per sample on average were removed from the analysis. To compute total number of reads per TE family/subfamily, counts on all integrants were summed using multi-mapping read counts with fractions (featureCounts with options -M –fraction -p -T 4 -t exon -g gene_id -Q 0) to compensate for potential bias in repetitive elements.

Differential gene expression analysis was performed using voom (Law et al., 2014) as implemented in the limma package of Bioconductor. A gene (or TE) was considered to be differentially expressed when the fold change between groups was greater than two and the *P*-value was less than 0.05. A moderated *t*-test (as implemented in the limma package of R) was used to test significance. *P*-values were corrected for multiple testing using the Benjamini–Hochberg method.

Acknowledgements

We thank the Transgenic Core Facility of EPFL for technical assistance.

Funding

This work was supported by grants from the European Research Council (KRABnKAP, No. 268721; Transpos-X, No. 694658) and the Swiss National Science Foundation (Schweizerischer Nationalfonds zur Förderung der Wissenschaftlichen Forschung).

References

Chen Z, Zhang Y. Loss of DUX causes minor defects in zygotic genome activation and is compatible with mouse development. Nat Genet. 2019; 51doi: 10.1038/s41588-019-0418-7

De Iaco A, Planet E, Coluccio A, Verp S, Duc J, Trono D. DUX-family transcription factors regulate zygotic genome activation in placental mammals. Nat Genet. 2017; 49:941–945. DOI: 10.1038/ng.3858 [PubMed: 28459456]

De Iaco A, Coudray A, Duc J, Trono D. DPPA2 and DPPA4 are necessary to establish a totipotent state in mouse embryonic stem cells. EMBO Rep. 2019; 20:e47382.doi: 10.15252/embr.201847382 [PubMed: 30948459]

Eckersley-Maslin M, Alda-Catalinas C, Blotenburg M, Kreibich E, Krueger C, Reik W. Dppa2 and Dppa4 directly regulate the Dux-driven zygotic transcriptional program. Genes Dev. 2019; 33:194–208. DOI: 10.1101/gad.321174.118 [PubMed: 30692203]

Gentleman RC, Carey VJ, Bates DM, Bolstad B, Dettling M, Dudoit S, Ellis B, Gautier L, Ge Y, Gentry J, et al. Bioconductor: open software development for computational biology and bioinformatics. Genome Biol. 2004; 5doi: 10.1186/gb-2004-5-10-r80

Guo M, Zhang Y, Zhou J, Bi Y, Xu J, Xu C, Kou X, Zhao Y, Li Y, Tu Z, et al. Precise temporal regulation of Dux is important for embryo development. Cell Res. 2019; 29:956–959. DOI: 10.1038/s41422-019-0238-4 [PubMed: 31591446]

Hendrickson PG, Doráis JA, Grow EJ, Whiddon JL, Lim JW, Wike CL, Weaver BD, Pflueger C, Emery BR, Wilcox AL, et al. Conserved roles of mouse DUX and human DUX4 in activating cleavage-stage genes and MERVL/HERVL retrotransposons. Nat Genet. 2017; 49:925–934. DOI: 10.1038/ng.3844 [PubMed: 28459457]

Jukam D, Shariati SAM, Skotheim JM. Zygotic genome activation in vertebrates. Dev Cell. 2017; 42:316–332. DOI: 10.1016/j.devcel.2017.07.026 [PubMed: 28829942]

Kim D, Langmead B, Salzberg SL. HISAT: a fast spliced aligner with low memory requirements. Nat Methods. 2015; 12:357–360. DOI: 10.1038/nmeth.3317 [PubMed: 25751142]

Law CW, Chen Y, Shi W, Smyth GK. voom: precision weights unlock linear model analysis tools for RNA-seq read counts. Genome Biol. 2014; 15doi: 10.1186/gb-2014-15-2-r29

Lee MT, Bonneau AR, Takacs CM, Bazzini AA, DiVito KR, Fleming ES, Giraldez AJ. Nanog, Pou5f1 and SoxB1 activate zygotic gene expression during the maternal-to-zygotic transition. Nature. 2013; 503:360–364. DOI: 10.1038/nature12632 [PubMed: 24056933]

Leidenroth A, Clapp J, Mitchell LM, Coneyworth D, Dearden FL, Iannuzzi L, Hewitt JE. Evolution of DUX gene macrosatellites in placental mammals. Chromosoma. 2012; 121:489–497. DOI: 10.1007/s00412-012-0380-y [PubMed: 22903800]

Liang H-L, Nien C-Y, Liu H-Y, Metzstein MM, Kirov N, Rushlow C. The zinc-finger protein Zelda is a key activator of the early zygotic genome in Drosophila. Nature. 2008; 456:400–403. DOI: 10.1038/nature07388 [PubMed: 18931655]

Liao Y, Smyth GK, Shi W. featureCounts: an efficient general purpose program for assigning sequence reads to genomic features. Bioinformatics. 2014; 30:923–930. DOI: 10.1093/bioinformatics/btt656 [PubMed: 24227677]

Madan B, Madan V, Weber O, Tropel P, Blum C, Kieffer E, Viville S, Fehling HJ. The pluripotency-associated gene Dppa4 is dispensable for embryonic stem cell identity and germ cell development but essential for embryogenesis. Mol Cell Biol. 2009; 29:3186–3203. DOI: 10.1128/MCB.01970-08 [PubMed: 19332562]

Nakamura T, Nakagawa M, Ichisaka T, Shiota A, Yamanaka S. Essential roles of ECAT15-2/Dppa2 in functional lung development. Mol Cell Biol. 2011; 31:4366–4378. DOI: 10.1128/MCB.05701-11 [PubMed: 21896782]

Snider L, Geng LN, Lemmers RJLF, Kyba M, Ware CB, Nelson AM, Tawil R, Filippova GN, van der Maarel SM, Tapscott SJ, et al. Facioscapulohumeral dystrophy: incomplete suppression of a retrotransposed gene. PLoS Genet. 2010; 6:e1001181.doi: 10.1371/journal.pgen.1001181 [PubMed: 21060811]

Whiddon JL, Langford AT, Wong CJ, Zhong JW, Tapscott SJ. Conservation and innovation in the DUX4-family gene network. Nat Genet. 2017; 49:935–940. DOI: 10.1038/ng.3846 [PubMed: 28459454]

Europe PMC Funders Author Manuscripts

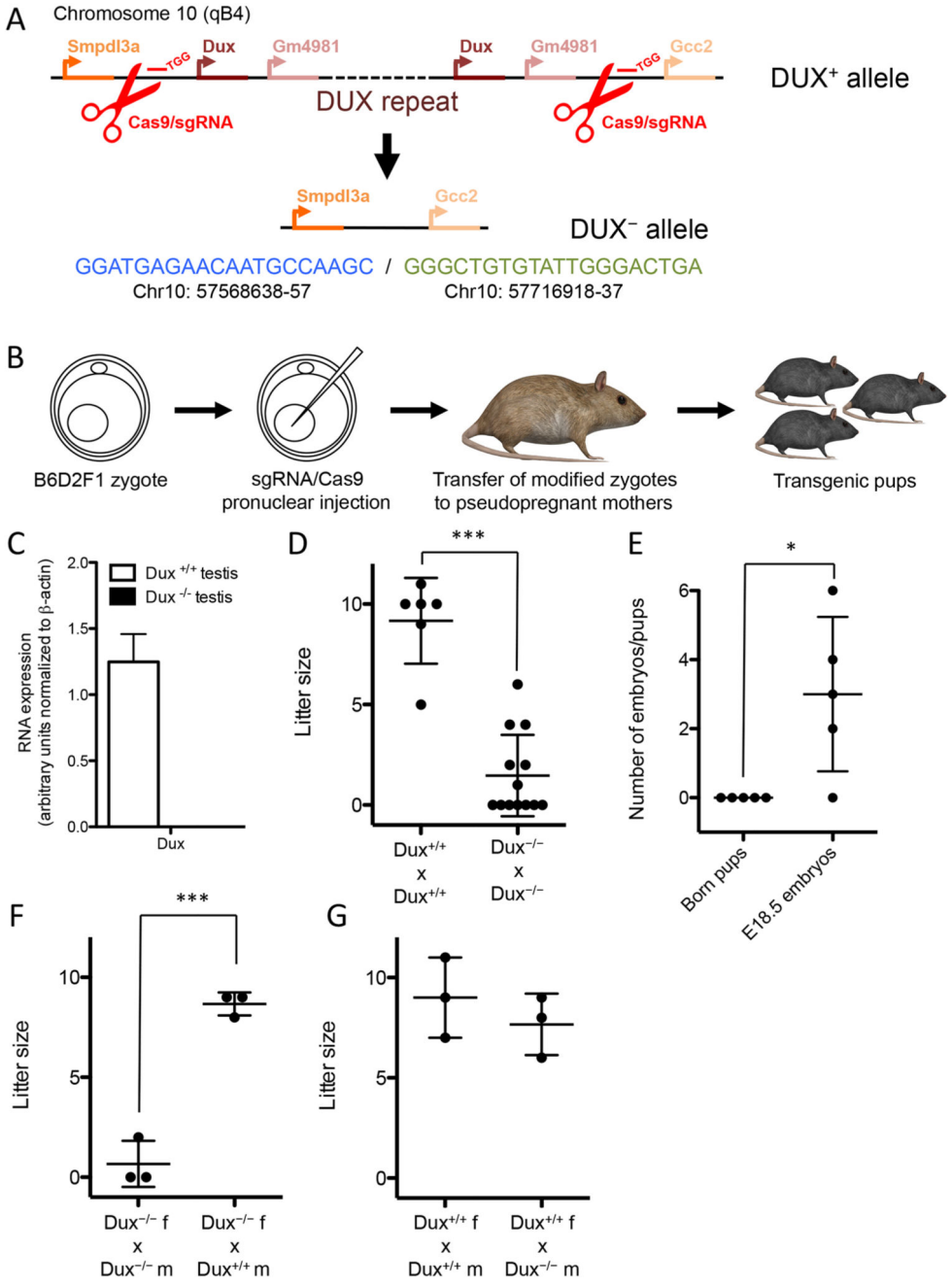

Fig. 1. DUX promotes embryonic development but is not necessary for it.

(A) Schematics of CRISPR/Cas9 depletion of *Dux* alleles. sgRNAs targeting the flanking region of the *Dux* repeat recruit Cas9 nucleases for the excision of the allele. *Dux* and *Gm4981* are two isoforms of the *Dux* gene repeated in tandem in the *Dux* locus. *Smpdl3a* and *Gcc2* are the genes flanking the *Dux* locus. The nucleotide sequence represents the exact junction of deletion determined by Sanger sequence. The sequences in blue and green represent, respectively, the DNA sequence upstream and downstream of the *Dux* deletion. (B) Generation of $Dux^{-/-}$ transgenic mice. Zygotes were injected in the pronucleus with

Europe PMC Funders Author Manuscripts

plasmids encoding for Cas9 nuclease and the specific sgRNAs, transferred to a pseudopregnant mother and the transgenic pups were finally screened for the null alleles. (C) Expression of *Dux* normalized to β-actin in testes from adult $Dux^{+/+}$ and $Dux^{-/-}$ mice. (D) WT or *Dux* KO parents were crossed and litter size was quantified. ***$P \leq 0.001$, two-tailed, unpaired *t*-test. (E) $Dux^{-/-}$ males and females were bred and the number of born pups was quantified. The same animals were bred again and embryos were quantified at E18.5. *$P \leq 0.05$, two-tailed, unpaired *t*-test. (F) $Dux^{-/-}$ females were crossed with $Dux^{-/-}$ or $Dux^{+/+}$ males and litter size was quantified. ***$P \leq 0.001$, two-tailed, unpaired *t*-test. (G) $Dux^{+/+}$ females were crossed with $Dux^{-/-}$ or $Dux^{+/+}$ males and litter size was quantified. In D-F, horizontal lines represent the average and error bars the s.d.

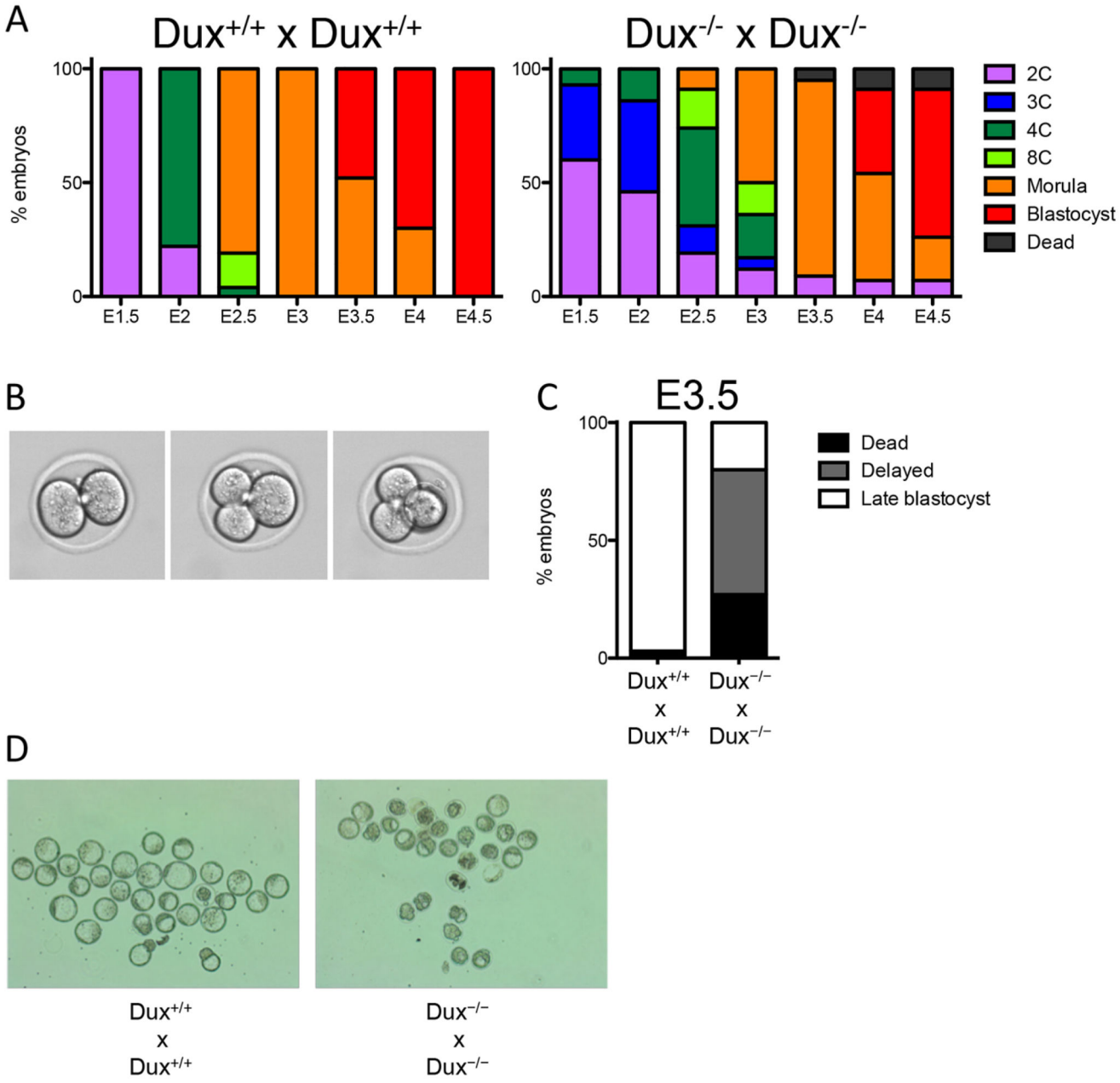

Fig. 2. *Dux* promotes both pre-implantation development and later stages.

(A) Zygotes from *Dux*$^{+/+}$ (n=3) or *Dux*$^{-/-}$ (n=5) parents were monitored every 12 h for their ability to differentiate *ex vivo* from E1.5 to E4.5. The average percentage of *Dux*$^{+/+}$ (n=27) or *Dux*$^{-/-}$ (n=42) embryos reaching a specific embryonic stage at each time point is represented. (B) *Dux*$^{-/-}$ embryos were monitored every hour for 68 h from zygote to morula. The brightfield images represent the unusual transition from 2C to 4C with a 3C intermediate. E3.5 embryos from WT (n=30) or *Dux* KO (n=28) parents were collected. (C) The average percentage of embryos reaching the late-blastocyst stages (white) or failing to differentiate (delayed embryos, gray; dead embryos, black) was quantified. (D) Brightfield images of the E3.5 embryos.

Europe PMC Funders Author Manuscripts

Europe PMC Funders Author Manuscripts

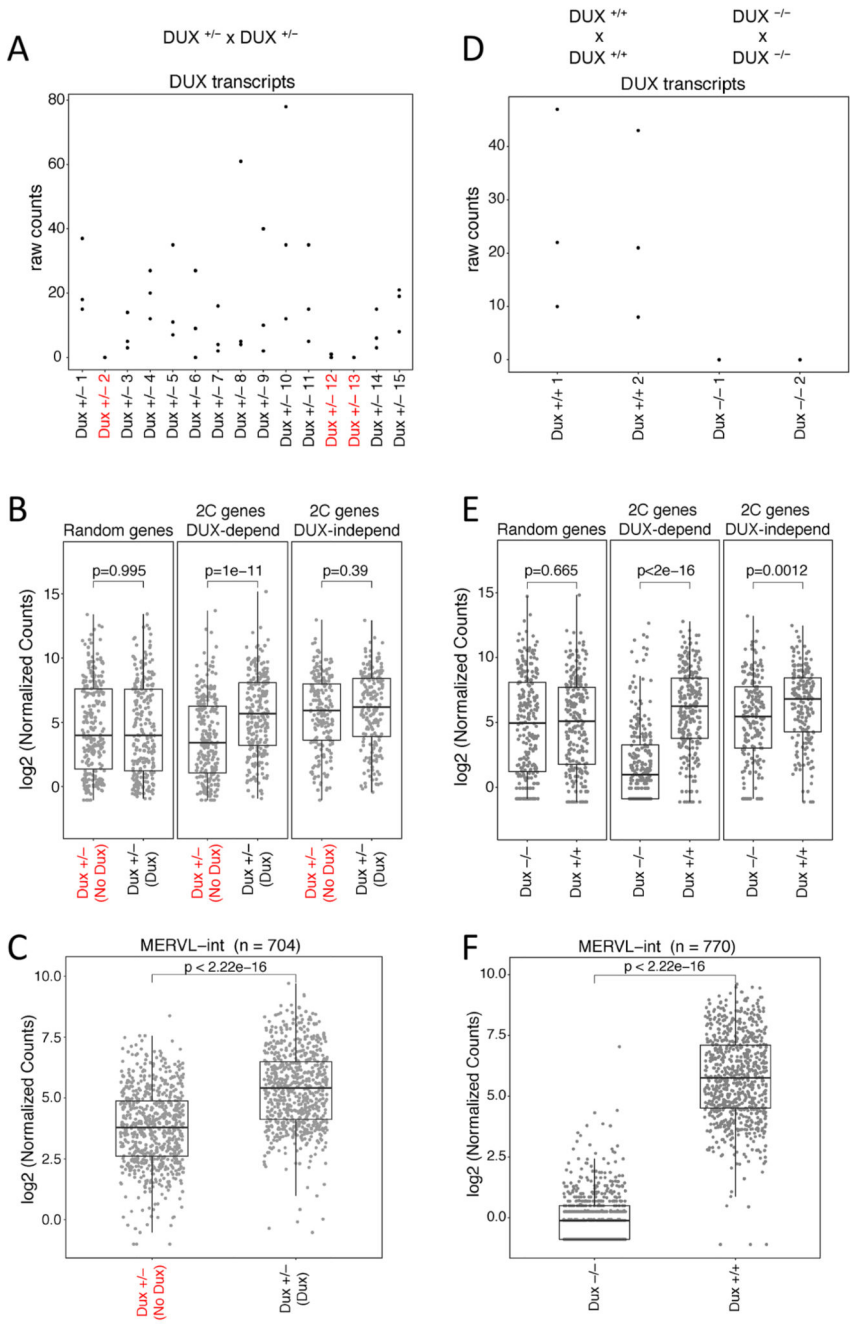

Fig. 3. Genes and TEs activated by DUX in mESCs are expressed at a low level in 2C embryos depleted of DUX.

(A-C) RNA sequencing analysis of 15 2C embryos generated by mating three *Dux*$^{+/-}$ males with three *Dux*$^{+/-}$ females. Transcription levels of (A) three alternative transcripts of *Dux*, (B) 2C-specific genes dependent or not on DUX expression in mESCs compared with a random set of genes, and (C) MERVL-int. In red are the putative *Dux*$^{-/-}$ embryos selected for the absence of expression of the three alternative transcripts of *Dux*. (D-F) RNA sequencing analysis of two embryos generated by mating *Dux*$^{+/+}$ mice and two embryos generated by mating *Dux*$^{-/-}$ mice. Transcription levels of (D) three alternative transcripts of

Dux, (E) putative DUX-dependent genes compared with a random set of genes, and (F) MERVL-int. Dots in B, C, E and F represents the mean expression (log2 normalized counts) of each gene in all embryos with the same genotype. Box limits, 25th and 75th percentiles; lines in the boxes, median. Whiskers are shown as implemented in the ggplot2 package of R. The upper whisker extends from the hinge to the largest value, no further than 1.5× the interquartile range (IQR) from the hinge. The lower whisker extends from the hinge to the smallest value, at most 1.5× the IQR of the hinge. *P*-value, two-tailed, unpaired *t*-test.

Europe PMC Funders Author Manuscripts

Europe PMC Funders Author Manuscripts

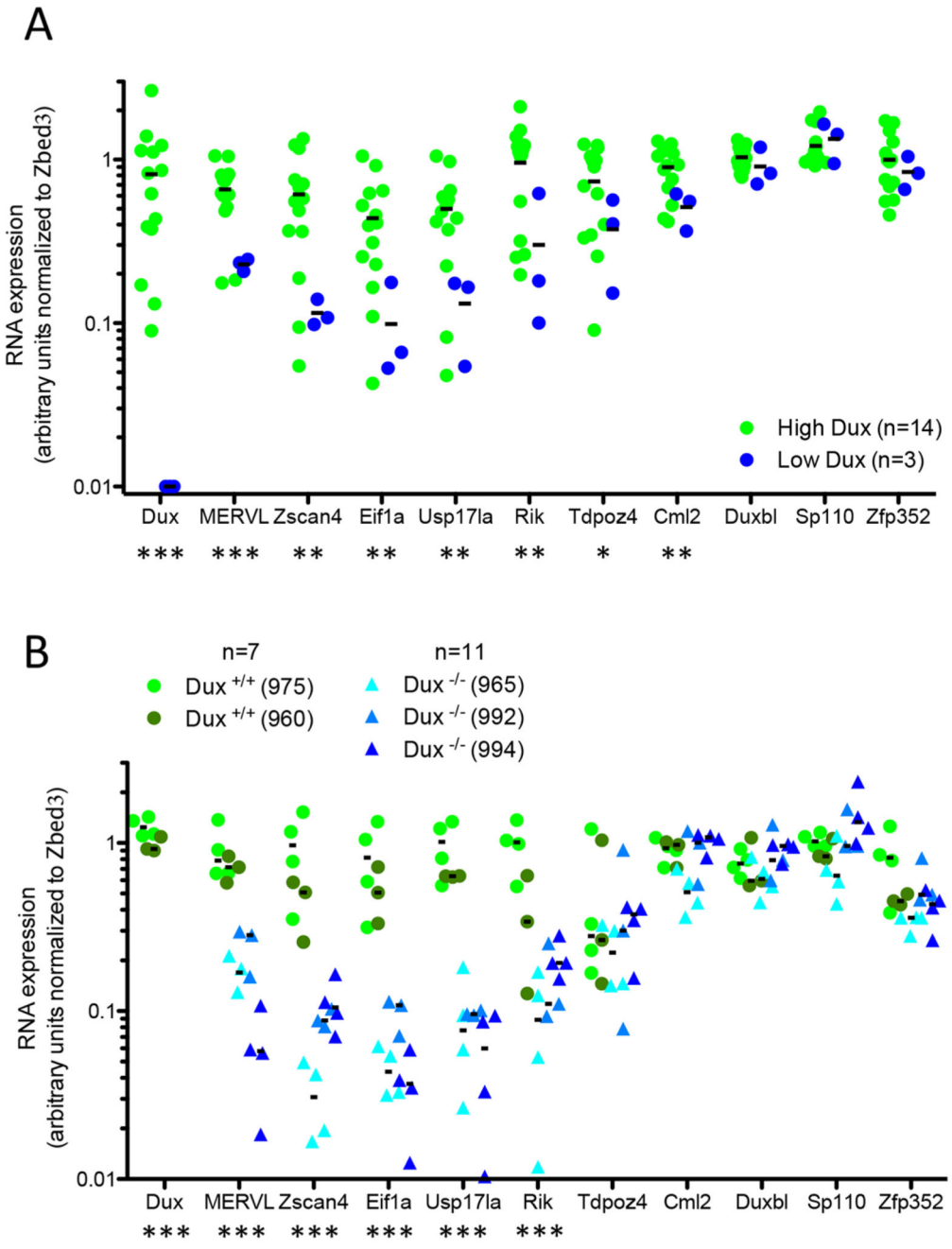

Fig. 4. Not all DUX target genes are downregulated in 2C embryos in the absence of DUX.

(A,B) Comparative expression of *Dux*, early ZGA genes [*Zscan4*, *Eif1a*, *Usp17la*, *B020004J07Rik* (Rik), *Tdpoz4*, *Cml2*, *Duxbl*, *Sp110*, *Zfp352*], a 2C-restricted TE (MERVL), normalized to *Zbed3*, a gene stably expressed during pre-implantation embryonic development, in 2C-stage embryos derived from (A) $Dux^{+/-}$ breeding (n=4) or (B) $Dux^{+/+}$ (n=2) and $Dux^{-/-}$ (n=3) breeding. Green and blue dots in A represent the mRNA levels of embryos expressing high or low levels of *Dux*, respectively. Different shades of green or blue in B represent embryos collected from different mothers (975 and 960 are $Dux^{+/+}$

mothers, 965, 992 and 994 are *Dux*$^{-/-}$ mothers). Horizontal black lines indicate average. *$P \leq$X.XXX, **$P \leq 0.01$, ***$P \leq 0.001$, two-tailed, unpaired *t*-test.

Europe PMC Funders Author Manuscripts

Europe PMC Funders Author Manuscripts

Table 1

Genotype distribution from *Dux*$^{+/-}$×*Dux*$^{+/-}$ crosses

Genotypes	*Dux*$^{+/+}$	*Dux*$^{+/-}$	*Dux*$^{-/-}$
Observed number of pups	118 (27%)	225 (52%)	93 (21%)
Expected number of pups	109 (25%)	218 (50%)	109 (25%)

Pearson's Chi-squared test: *P*-value=0.22.

Europe PMC Funders Author Manuscripts

Table 2

Genotype distribution from *Dux*$^{+/+}$×*Dux*$^{+/+}$ and *Dux*$^{-/-}$×*Dux*$^{-/-}$crosses

Crosses	*Dux*$^{+/+}$×*Dux*$^{+/+}$	*Dux*$^{-/-}$×*Dux*$^{-/-}$
Total number of pups (number of litters)	55 (6)	36 (17)***
Average litter size	9.2	2.1
Day of delivery (E)	19.5	20.8***

*** $P \leq 0.001$, two-tailed, unpaired *t*-test.